

See discussions, stats, and author profiles for this publication at: <https://www.researchgate.net/publication/6821358>

# Pt Nanoparticles: Heat Treatment–Based Preparation and Ru(bpy)<sub>3</sub><sup>2+</sup>–Mediated Formation of Aggregates That Can Form Stable Films on Bare Solid Electrode Surfaces for Solid–State El...

ARTICLE in ANALYTICAL CHEMISTRY · OCTOBER 2006

Impact Factor: 5.64 · DOI: 10.1021/ac060325j · Source: PubMed

---

CITATIONS

37

---

READS

145

5 AUTHORS, INCLUDING:



**Xuping Sun**

Chinese Academy of Sciences

268 PUBLICATIONS 7,907 CITATIONS

SEE PROFILE



**Judy Du**

University of Ottawa

27 PUBLICATIONS 845 CITATIONS

SEE PROFILE



**Lixue Zhang**

Chinese Academy of Sciences

40 PUBLICATIONS 1,072 CITATIONS

SEE PROFILE

## Correspondence

# Pt Nanoparticles: Heat Treatment-Based Preparation and Ru(bpy)<sub>3</sub><sup>2+</sup>-Mediated Formation of Aggregates That Can Form Stable Films on Bare Solid Electrode Surfaces for Solid-State Electrochemiluminescence Detection

Xuping Sun, Yan Du, Lixue Zhang, Shaojun Dong,\* and Erkang Wang\*

State Key Laboratory of Electroanalytical Chemistry, Changchun Institute of Applied Chemistry, Chinese Academy of Sciences, Graduate School of the Chinese Academy of Sciences, Changchun, Jilin 130022, P. R. China

A simple thermal process for the preparation of small Pt nanoparticles is presented, carried out by heating a H<sub>2</sub>-PtCl<sub>6</sub>/3-thiophenemalonic acid aqueous solution. The following treatment of such colloidal Pt solution with Ru(bpy)<sub>3</sub><sup>2+</sup> causes the assembly of Pt nanoparticles into aggregates. Most importantly, directly placing such aggregates on bare solid electrode surfaces can produce very stable films exhibiting excellent electrochemiluminescence behaviors.

Metal nanoparticles have found applications in many fields due to their novel electronic, optical, thermal, and catalytic properties,<sup>1</sup> and their syntheses have thus attracted considerable attention.<sup>2</sup> Ruthenium(II) tris(bipyridine) (Ru(bpy)<sub>3</sub><sup>2+</sup>) is one of the most extensively studied and used electrochemiluminescence (ECL) compounds due to its superior properties including high sensitivity and high stability under moderate conditions in aqueous solution,<sup>3</sup> and considerable attention has been paid to the immobilization of Ru(bpy)<sub>3</sub><sup>2+</sup> on electrode surfaces, aiming at developing cost-effective, regenerable, chemical sensors and biosensors.<sup>4</sup> To date, many approaches for effective immobilization of Ru(bpy)<sub>3</sub><sup>2+</sup> on solid electrode surfaces have been developed, including the immobilization of Ru(bpy)<sub>3</sub><sup>2+</sup> in polymer layers on electrode surfaces, the direct attachment of Ru(bpy)<sub>3</sub><sup>2+</sup> to an electrode as a monolayer by a Langmuir–Blodgett technique or by a self-assembly technique, and the fabrication of multilayers of Ru(bpy)<sub>3</sub><sup>2+</sup> on electrode surfaces by layer-by-layer technique.<sup>4,5</sup> More recently, we have developed a simple method for effective

immobilization of Ru(bpy)<sub>3</sub><sup>2+</sup> involving the formation of aggregates of citrate-capped gold nanoparticles and Ru(bpy)<sub>3</sub><sup>2+</sup> in aqueous solution and the following attachment of such aggregates on sulfhydryl-derived indium tin oxide (ITO) electrode surfaces. We found that the modification of substrate with sulfhydryl group and the resultant strong Au–S interactions between sulfhydryl group and gold nanoparticles are crucial to the effective immobilization of the aggregates and there is no stable film formed on bare ITO surfaces.<sup>6</sup>

In this correspondence, we demonstrate that heating a H<sub>2</sub>-PtCl<sub>6</sub>/3-thiophenemalonic acid (TA) aqueous solution gives stable, small Pt nanoparticles and the following treatment of such particles with Ru(bpy)<sub>3</sub><sup>2+</sup> in aqueous solution causes the assembly of such particles into aggregates. Most importantly, directly placing such aggregates on bare solid electrode surfaces can produce very stable films exhibiting excellent electrochemiluminescence behaviors.

## EXPERIMENTAL SECTION

**Reagents.** H<sub>2</sub>PtCl<sub>6</sub>, TA, and Ru(bpy)<sub>3</sub>Cl<sub>2</sub>·6H<sub>2</sub>O were purchased from Aldrich. All reagents were used as received without further purification. The water used was purified through a Millipore system.

**Preparation of Pt Nanoparticles.** Pt nanoparticles were prepared by heating a H<sub>2</sub>PtCl<sub>6</sub>/TA aqueous solution: In brief, 2 mL of 0.038 M H<sub>2</sub>PtCl<sub>6</sub> aqueous solution was diluted to 100 mL with water first, and then 1 mL of 0.3 M TA was added into the solution. As-formed solution was heated at 100 °C for 20 min, giving a dark brown solution.

**Preparation of Aggregates.** Aggregates were prepared by treating the colloidal Pt solution with Ru(bpy)<sub>3</sub><sup>2+</sup> aqueous solution: In brief, 1 mL of 0.038 M Ru(bpy)<sub>3</sub>Cl<sub>2</sub> aqueous solution was slowly added into 50 mL of as-prepared colloidal Pt solution under vigorous stirring. Several minutes later, a large quantity of black aggregates occurred and precipitated.

\* To whom correspondence should be addressed. Fax: (+86) 431-5689711. E-mail: dongsj@ciac.jl.cn; ekwang@ciac.jl.cn.

- (1) Fendler, J. H. *Nanoparticles and nanostructured films*; VCH: Weinheim, 1998.
- (2) Schmid, G. *Chem. Rev.* **1992**, 92, 1709.
- (3) Honda, K.; Yoshimura, M.; Rao, T. N.; Fujishima, A. *J. Phys. Chem. B* **2003**, 107, 1653.
- (4) Guo, Z.; Shen, Y.; Wang, M.; Zhao, F.; Dong, S. *Anal. Chem.* **2004**, 76, 184.
- (5) See, for example: (a) Rubinstein, I.; Bard, A. J. *J. Am. Chem. Soc.* **1980**, 102, 6641. (b) Lyons, C. H.; Abbas, E. D.; Lee, J.-K.; Rubner, M. F. *J. Am. Chem. Soc.* **1998**, 120, 12100.

(6) Sun, X.; Du, Y.; Dong, S.; Wang, E. *Anal. Chem.* **2005**, 77, 8166.

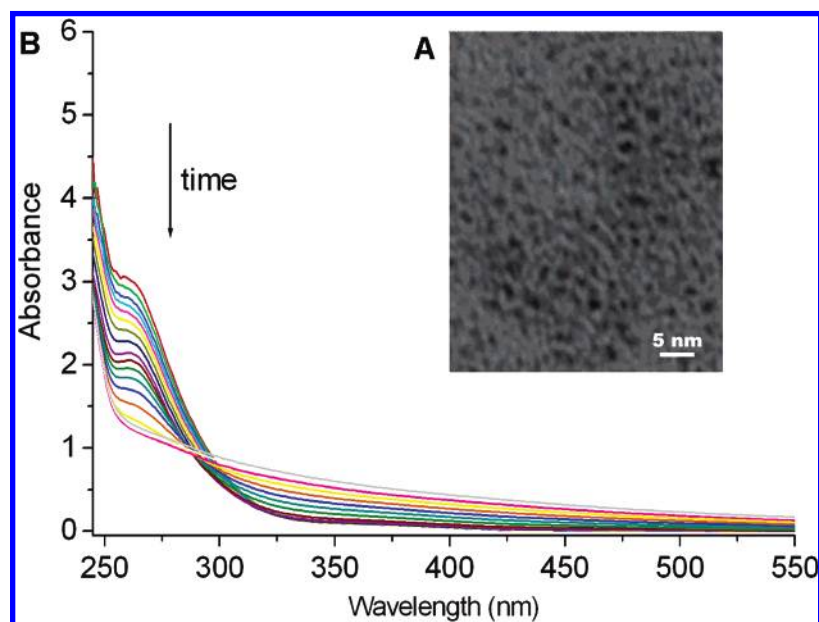


**Figure 1.** (A) TEM image of the resulting Pt nanoparticles. (B) Time-dependent UV–visible spectra of a  $\text{H}_2\text{PtCl}_6/\text{TA}$  aqueous solution heated at  $100^\circ\text{C}$  with time interval of 1 min.

**Immobilization of the Aggregates on Bare Solid Electrode Surfaces.** A  $10\text{-}\mu\text{L}$  sample of the suspension of the aggregates in water was placed on bare indium tin oxide (ITO) or other electrode surfaces and air-dried at room temperature, followed by thorough rinsing of the film formed on the electrode surfaces with water.

**Instrument.** Samples for transmission electron microscopy (TEM) characterization were prepared by placing a drop of gold colloidal Pt solution onto a carbon-coated copper grid and drying at room temperature. TEM measurements were made on a JEOL 2010 transmission electron microscopy. Samples for scanning electron microscopy (SEM) and electrochemical characterization were prepared by placing  $20\text{ }\mu\text{L}$  of the suspension of the aggregates in water on an ITO glass slide and air-drying at room temperature. SEM measurements were made on a XL30 ESEM FEG scanning electron microscopy. UV–visible spectra were collected on a Cary 500 Scan UV–vis–near-infrared (UV–visible–NIR) spectrophotometer. XPS was collected on an Esclab MKII. Cyclic voltammetry experiments were made on a model 800 electrochemical analyzer, and ECL signals were monitored by a MCFL-A multifunctional chemiluminescent and bioluminescent analytical system.

## RESULTS AND DISCUSSION

Figure 1A shows the TEM image of Pt nanoparticles thus formed. It is clear that nanoparticles thus formed are small ( $<2\text{ nm}$ ); however, we cannot determine the exact particle diameter from the TEM observation. XPS was used to identify the change in oxidation states for Pt after the heat treatment had occurred (Figure S1, Supporting Information). The binding energy of the Pt products shows two binding energy peaks of the Pt 4f region at 71.8 and 75.4 eV, confirming the formation of metallic Pt.<sup>7</sup> The formation process of the Pt nanoparticles during the thermal

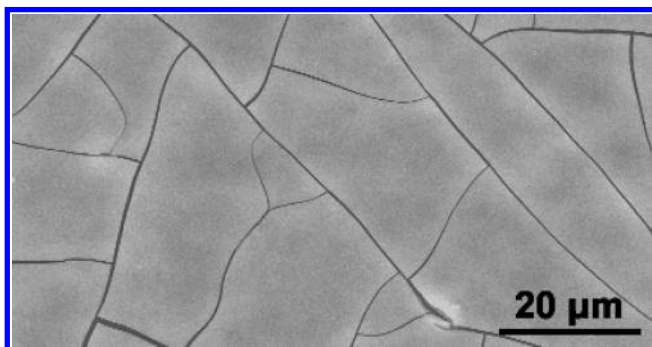
process was further traced by time-dependent UV–visible spectra (Figure 1B). With the elapsed time, the peak at 258 nm gradually disappears, suggesting a gradual reduction of  $\text{PtCl}_6^{2-}$ , and finally, this peak completely disappears and we observe a spectrum that has absorption in all ranges of the UV–visible spectrum studied and the absorption increases gradually with the decrease of wavelength, indicating that the  $\text{PtCl}_6^{2-}$  ions have been completely reduced to form Pt nanoparticles.<sup>8</sup> The formation of such Pt nanoparticles can also be attributed to the direct redox between TA and  $\text{PtCl}_6^{2-}$ , because there are no other reducing reagents in the solution. Note that such Pt nanoparticles were stable for several months without any observable aggregation, indicating that TA serves as a very effective protective agent for the formation of Pt nanoparticles, which can be attributed to the fact the sulfur atom in TA has a very strong nucleophilicity with lone-pair electrons and such a lone-pair electron can form a type of donor–acceptor complex with the Pt atom on the particle surface, yielding TA-protected Pt nanoparticles.

Figure 2 shows an SEM image of the resulting aggregates coated on an ITO substrate, indicating that the aggregates form a fairly smooth film on the substrate. Many cracks are also observed, which may result from the high surface tension arising during solvent evaporation. The chemical composition of the aggregates was examined by the energy-dispersed spectrum (EDS) (Figure S2, Supporting Information). The peaks of Pt, C, N, O, S, and Ru are found (other peaks originated from the ITO substrate), indicating the aggregates are formed from TA-protected Pt nanoparticles and  $\text{Ru}(\text{bpy})_3^{2+}$ . Considering the acidic reaction condition, the Pt particle surface is mainly covered by protonated carboxylic acid groups and thus the electrostatic interactions between positively charged  $\text{Ru}(\text{bpy})_3^{2+}$  and Pt nanoparticles<sup>9</sup> are only partially responsible for the formation of the aggregates. On the other hand, both TA and  $\text{Ru}(\text{bpy})_3^{2+}$  are rich

(7) Drawdy, E.; Hoflund, G. B.; Gardner, S. D.; Yngvadottir, E.; Schryer, D. R. *Surf. Interface Anal.* **1990**, *16*, 369.

(8) Teranishi, T.; Hosoe, M.; Tanaka, T.; Miyake, M. *J. Phys. Chem. B* **1999**, *103*, 3818.

(9) Shipway, A. N.; Lahav, M.; Gabai, R.; Willner, I. *Langmuir* **2000**, *16*, 8789.



**Figure 2.** SEM image of the resulting aggregates coated on an ITO substrate.

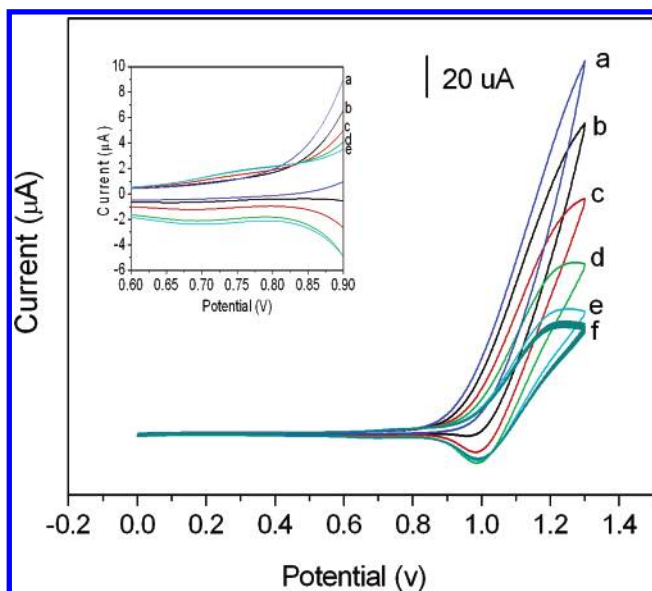


**Figure 3.** CVs of as-formed film on an ITO substrate in 50 mM phosphate buffer solution (pH 7.5; curves a–e corresponding to cycles 1, 5, 10, 15, and 20, respectively) at scan rate 50 mV/s. Inset: a local magnification image. Curve f corresponding to the CVs after 25 cycling scans.

in  $\pi$ -type bonds and the strong intermolecular  $\pi$ - $\pi$  interactions between them also contribute to the formation of the aggregates via self-assembly.<sup>10</sup>

Figure 3 shows the cyclic voltammograms (CVs) of the as-formed film on an ITO substrate at a scan rate 50 mV/s in 50 mM phosphate buffer solution. During the first several scans, the current steeply goes up after 0.9 V and no peak occurs. However, a pair of redox waves characteristic of  $\text{Ru}(\text{bpy})_3^{2+}$  with an oxidation peak at 1.18 V and a reduction peak at 1.0 V (vs Ag/AgCl) appears when 15 cycling scans are applied (curve d).<sup>4</sup> Note that it is the case for the first 25 cycling scans that the oxidation current decreases but the reduction current increases (from curve a to f) and the redox peak separation decreases from 180 to 120 mV. After that, stable CVs are observed. Figure S3 (Supporting Information) shows the ECL intensity–time curve corresponding to the first 29 cycling scans. It is found that the ECL signal of the first 26 cycling scans gradually increases, which may be attributed to the following two facts: (1) the  $\text{Ru}(\text{bpy})_3^{2+}$  species contained in the film can wholly be involved in the ECL reaction only after a period of potential cycling;

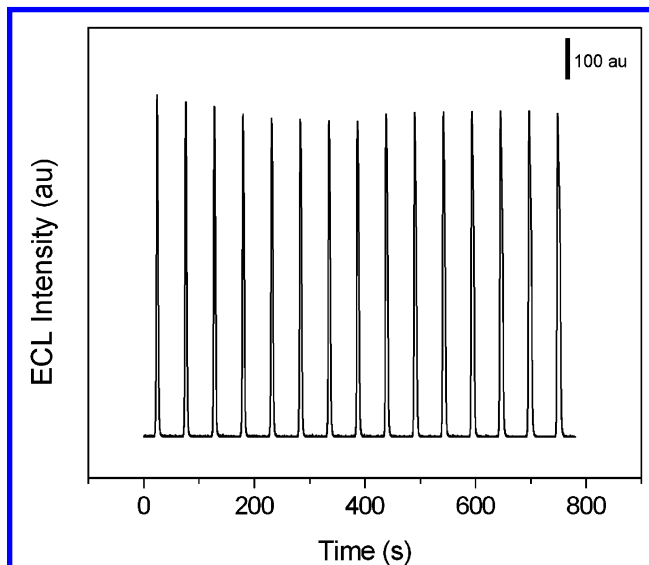


**Figure 4.** Corresponding ECL intensity–time curve of as-formed film on an ITO substrate under continuous potential scanning from the 30th to 45th cycling scans (pH 7.5) at scan rate 50 mV/s.

(2) some aggregates contained in the film are loosely bound to the electrode surface and gradually fall from the surface during the first potential cycling. As a result, the film becomes much looser, and therefore, both a more facile electron transfer between the  $\text{Ru}(\text{bpy})_3^{2+}$  in the film and the electrode surface and an easier diffusion of OH in solution into the film occur. Consequently, the intensity of ECL signal gradually increases. After that, a quite stable ECL signal ( $\sim 800$  au) is observed, which can be evidenced by Figure 4. It suggests that a stable film is finally formed. Because  $\text{Ru}(\text{bpy})_3^{2+}$  is the only luminescent component in the film, it is expected that the luminescence observed results from the reaction of  $\text{Ru}(\text{bpy})_3^{2+}$  with OH.<sup>6</sup> Figure S4 (Supporting Information) shows the ECL intensity–time curve of the film in the absence and presence of 50  $\mu\text{M}$  tripropylamine (TPA). Obviously, the addition of TPA remarkably increases the ECL intensity (from  $\sim 800$  to  $\sim 4800$  au). All these observations indicate that the film is quite stable and the  $\text{Ru}(\text{bpy})_3^{2+}$  components in the film still exhibit good electrochemical activity and excellent ECL behavior. Note that the film is quite stable on any other bare electrode surfaces such as glassy carbon, graphite, Au, and Pt electrode.

The formation of the stable film of the aggregates on a bare electrode surface can be attributed to the fact that the TA in the aggregates is electrochemically polymerized during the cycling scans to form stable polymer film on electrode surface<sup>11</sup> and the polymer film can effectively protect the aggregates from falling from the electrode surface. The fact that a pair of wave waves  $\sim 0.7$  V also gradually appear (inset in Figure 3) during the cycling process confirms the formation of the polymers when cycling potentials are applied.<sup>12</sup> During the first several scans, no stable polymer film is formed and some aggregates have fallen from the electrode surface. As a result, the oxidation current declines continuously with potential cycling. When a stable polymer film is formed with further cycling scans,

(11) Mu, S.; Park, S.-M. *Synth. Met.* **1995**, *69*, 311.

(12) Thackeray, J. W.; White, H. S.; Wrighton, M. S. *J. Phys. Chem.* **1985**, *89*, 5133.

(10) Sun, X.; Dong, S.; Wang, E. *Macromol. Rapid Commun.* **2005**, *26*, 1504.

no aggregates have fallen from the electrode surface, and therefore, stable CVs and ECL signals are observed, indicating the formation of a stable film of aggregates on the electrode surface.

## CONCLUSIONS

We demonstrate a simple thermal strategy for the preparation of stable, small Pt nanoparticles. The formation of Pt particles occurs in a single process, carried out by heating a  $\text{H}_2\text{PtCl}_6/\text{TA}$  aqueous solution. The following treatment of such particles with  $\text{Ru}(\text{bpy})_3^{2+}$  in aqueous solution causes the assembly of such particles into aggregates. Most importantly, directly placing such aggregates on bare solid electrode surfaces can produce very stable films exhibiting excellent electrochemiluminescence behaviors. Our finding is significant for the following two reasons: (1) It provides a general methodology for the preparation of noble metal nanoparticles for applications. (2) Such assemblies will

provide us new kind of materials for solid-state ECL detection in capillary electrophoresis (CE) or a CE microchip.

## ACKNOWLEDGMENT

This work was supported by the National Natural Science Foundation of China (20275036, 20275037, 20299030, 20210506).

## SUPPORTING INFORMATION AVAILABLE

XPS spectrum of Pt 4f region of the Pt nanoparticles; EDS of the aggregates; ECL intensity–time curve corresponding to the first 29 cycling scans of the film; ECL intensity–time curve of the stable film in the absence and presence of tripropylamine. This material is available free of charge via the Internet at <http://pubs.acs.org>.

Received for review February 22, 2006. Accepted July 20, 2006.

AC060325J